Peer-reviewed version available at *Energies* **2019**, *12*, 1901; doi:10.3390/en12101901

Article

Optimal sizing procedure for Electric Vehicle Supply Infrastructure based on DC microgrid with station commitment

Benedetto Aluisio, Maria Dicorato*, Imma Ferrini, Giuseppe Forte, Roberto Sbrizzai, Michele Trovato

Department of Electrical and Information Engineering, Politecnico di Bari, Bari, Italy
* Correspondence: maria.dicorato@poliba.it

Abstract: The diffusion of electric vehicles (EVs) can be sustained by the presence of integrated solutions offering parking and clean power supply. The recourse to DC systems allows to better integrate EV bidirectional energy exchange, photovoltaic panels and energy storage. In this paper, a methodology for optimal techno-economic sizing of a DC-microgrid for covering EV mobility needs is carried out. It is based on the definition of different scenarios of operation, according to typical EV usage outlooks and environmental conditions. In each scenario, optimal operation is carried out by means of a specific approach for EV commitment on different stations. The sizing procedure is able to handle the modular structure of microgrid devices. The proposed approach is applied to a case study of envisaged EV service fleet for Bari port authority.

Keywords: DC microgrid; electric vehicles; optimal sizing; station commitment.

---

1. Introduction

The spreading of electric vehicles (EVs) can represent a powerful mean to cope with mobility needs and realize a diversification of transport energy use with a lower carbon footprint [1]. In order to bolster the diffusion of EVs among end-users (e.g. residential, commuters, company fleets), along with selling price reduction, the presence of charging stations represents the most remarkable aspect [2]. However, to avoid demand peaks given by the presence of several EVs at the same time (e.g. at work arrival, or at homecoming), the charge process should be planned, supervised and controlled through a smart charging strategy [3][4]. The exploitation of vehicle-to-grid (V2G) is useful to cope with this necessity, where the EVs can act as a mobile energy storage device and even feed one another [5].

Photovoltaic (PV) technology is particularly suitable for integration with EV charging stations [6], by realizing canopies to host PV panels and provide for shaded vehicle parking [7][8]. The integration of PV and EV charging station has been proposed in several works, e.g. charge/discharge models of EVs in the presence of PV are analysed in [9], and in [10] economic models are developed for EV and parking owner perspectives under parking fee policies. Effects on regional basis are analysed in [11]. In order to reduce the EV impact on the network, the integration of energy storage systems (ESS) in EV charging station can be useful [12], with the aim of shifting power exchange according to price signals, smoothing out time variations [13].

The integration of those elements (EVs, charging points with V2G, PV systems, ESS) can constitute an Electric Vehicle Supply Infrastructure (EVSI) with a microgrid outline. This structure, introduced in previous works [16][17], can reveal particularly suitable for managing a fleet of corporate EVs, for instance in a small/medium enterprise or in a public entity. In this context, proper control strategies should be implemented involving smart charging, economic dispatch, real-time voltage control and islanding [14][15]. Moreover, all the mentioned EVSI components can be directly integrated in a DC-microgrid architecture, reducing AC/DC converter employment [18][19][20].

Peer-reviewed version available at Energies 2019, 12, 1901; doi:10.3390/en12101901

A research activity is open on the integration of EV-based microgrid, and operation planning strategies are investigated with different grid exchange objectives [15][22][23]. However, since the investment in EVs and relevant charging systems is still a major concern, a particular care is devoted to the sizing of an EV-based microgrid. This problem has been faced combining PV and EVs in [14], and considering the presence of a single ESS and EVs in [24] where network limits are studied and cost items are detailed for AC and DC configurations. Moreover, in [25] optimal sizing is determined and investment cost sensitivity is analysed, in [26] design criteria are discussed for fast charging station with ESS and PV for an EV fleet and operation is tested over a week, and in [27] optimal sizing including probabilistic solar production and queueing model of EVs is carried out.

In this paper, a procedure for techno-economic evaluation for DC microgrid configuration of EVSI is carried out. The procedure is intended to reduce economical efforts for investment and lifetime management of the microgrid. In particular, realistic spatial and technical limitations are taken into account, along with different operating conditions based on EV needs and availability of non-programmable renewable sources. The analysed configuration involves feasible combinations of converters as well as modular PV panels, ESS elements and EV charging stations, with a proper interface with the low-voltage AC distribution network. The proposed procedure is applied to the sizing of the microgrid that will be realized in the area of Bari Port Authority (Italy).

The main contributions of the paper can be individuated as follows:

- A mixed-integer procedure for EV-based microgrid optimal sizing and operation is provided, to cope with the modularity of microgrid components;
- A specific EV commitment is developed, in order to plan the station to which each EV should be connected;
- In order to draw the influence of DC microgrid layout, two different configurations are analysed on a realistic test case.

The paper is organized as follows. In Section 2, the proposed DC microgrid configurations are illustrated, and the formulation of the proposed methodology for DC microgrid optimal sizing and operation is described. In Section 3, the input data for the test case are presented. Simulation results are illustrated and discussed in Section 4. Conclusions are reported in Section 5.

2. DC microgrid optimal sizing methodology

For the complete list of symbols and their meaning, please refer to the Nomenclature at the end of the paper.

2.1. DC microgrid configurations

In order to carry out the sizing procedure, the proposed configurations for DC microgrid of the EVSI are considered. The Configuration, briefly discussed in [17], is depicted in Figure 1. It involves a bidirectional AC/DC converter for grid connection at Point of Common Coupling (PCC), monodirectional DC/DC converter with MPPT functionality for the integration of PV system, a bidirectional DC/DC converter for the ESS and different bidirectional DC/DC converters for the EV charging stations, in order to enable V2G performances. All the converters, including relevant protection devices, are connected to a common DC busbar at proper voltage level. Moreover, suitable internal collection systems for the input of PV panel strings to the converter and for the ESS modules are provided.

Peer-reviewed version available at Energies 2019, 12, 1901; doi:10.3390/en12101901

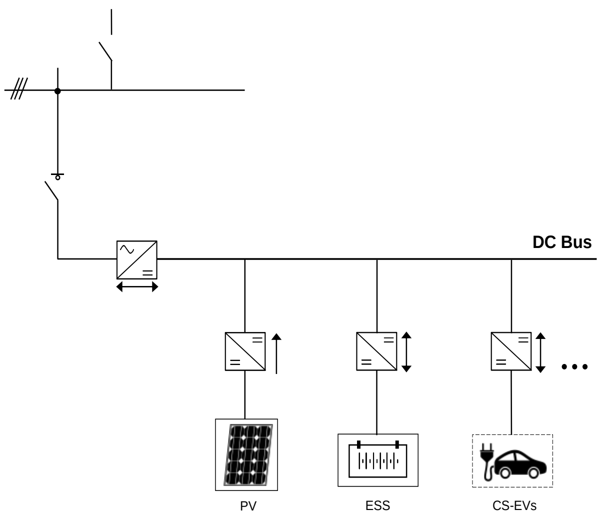

Figure 1. Configuration for the DC-based microgrid.

2.2. Modeling of EVSI components

The EVSI can include Np PV technologies, Ni ESS technologies and is able to exchange power with Nj EVs through Nk stations, where a set of Nr standards can be chosen. The behavior of each component is described by proper models for each *t*-th time step in the *s*-th scenario.

In order to assess the operation of the microgrid in the presence of different frameworks for vehicle use and generation availability, a scenario-based procedure is considered [28][29]. Since solar power production depends on weather conditions and seasons, and storage devices and EVs can show different use in weekdays as well as in subperiods of the year, a certain number Ns of scenarios, i.e. typical days, are defined in advance, considering that each *s*-th scenario can be observed for a given number of times D_s during the year.

2.2.1. PV systems

The power output of the *p*-th PV system depends on the available solar radiation and technological features, by means of the following expression:

$$P_{p,s,t} = R_p \cdot \frac{\eta_{p,s,t} \cdot G_{p,s,t}}{\eta_p^{std}} . \tag{1}$$

Since the relation (1) linearly links power output with the installed power R_p according to solar radiation $G_{p,s,t}$, $P_{p,s,t}$ is not included in state variables. In (1), the efficiency of the *p*-th PV system, $\eta_{p,s,t}$, is related to the forecasted weather conditions. Moreover, the incident solar radiation $G_{p,s,t}$ is estimated according to proper model starting from total radiation forecast on horizontal plane [30].

The PV installation is limited by available surface of parking roofs and should ensure shadowing for all the parking places next to EV charging stations:

$$\sum_{k \in \Omega k} S_k \le \sum_{p \in \Omega p} \frac{R_p}{\eta_p^{std}} \le S^{tot} . \tag{2.a}$$

Moreover, since PV system is made up by discrete modules, the installed power of the *p*-th PV technology to the number n_p of PV modules, according to the unit power of the module, by the following equality constraint:

Peer-reviewed version available at Energies 2019, 12, 1901; doi:10.3390/en12101901

$$R_p = n_p \cdot M_p \,. \tag{2.b}$$

Finally, the size of PV converter should be not less than the installed power of the PV system, and only one converter per each PV technology has to be installed.

$$P_{p,s,t} \le \sum_{m \in \Omega m} W_m \cdot b_{m,p} \,. \tag{2.c}$$

$$\sum_{m \in \Omega m} b_{m,p} \le 1 \,. \tag{2.d}$$

2.2.2. Energy storage systems

The behaviour of ESSs is characterized by SOC variation due to charging/discharging process with proper efficiencies. The following relation holds for the t-th time step:

$$E_{i,s,t} = E_{i,s,t-1} + \Delta t \cdot \left(\eta_i^c \cdot P_{i,s,t}^c - \frac{P_{i,s,t}^d}{\eta_i^d} \right) - z_i \cdot R_i \,, \tag{3.a}$$

where $E_{i,s,t-1}$ represents the SOC of the i-th ESS in the previous time step of the s-th scenario. For $t = 1$, $E_{i,s,0}$ represents the imposed SOC initial condition. Moreover, the SOC at $t = Nt$ is imposed equal to the initial condition, allowing to replicate the behaviour for consecutive days, i.e.:

$$E_{i,s,N_t} = E_{i,s,0} \,. \tag{3.b}$$

Technical limits of the i-th ESS are accounted by means of constraints on charge power, discharge power and SOC, depending on installed amount R_i:

$$0 \le P_{i,s,t}^c \le \frac{R_i}{\varphi_i^c} \cdot b_{i,s,t} \,. \tag{4.a}$$

$$0 \le P_{i,s,t}^d \le \frac{R_i}{\varphi_i^d} \cdot \left(1 - b_{i,s,t}\right) . \tag{4.b}$$

$$\underline{e}_i \cdot R_i \le E_{i,s,t} \le \overline{e}_i \cdot R_i \,. \tag{4.c}$$

The total installation of ESSs is limited by available volume for hosting the devices:

$$\sum_{i \in \Omega i} \delta_i \cdot R_i \le V^{tot} \,. \tag{5.a}$$

Analogously to PV system, the following equality constraints link the installed size of the i-th ESS to the number n_i of modules, according to the unit size of the chosen battery, and to the size of the converter:

$$R_i = n_i \cdot M_i \,. \tag{5.b}$$

$$R_i \le \sum_{h \in \Omega h} W_h \cdot \varphi_i^d \cdot b_{h,i} \,. \tag{5.c}$$

$$\sum_{h \in \Omega h} b_{h,i} \le 1 \,. \tag{5.d}$$

2.2.3. Electric vehicles and stations

EVs are dealt with as storage devices, as long as they are connected to a station. The relation for SOC update is valid for the t-th time step between $\tau_{j,s}^A + 1$ and $\tau_{j,s}^L$:

Preprints (www.preprints.org) | NOT PEER-REVIEWED | Posted: 22 March 2019

Peer-reviewed version available at Energies 2019, 12, 1901; doi:10.3390/en12101901

$$E_{i,s,N_t} = E_{i,s,0}, \tag{6}$$

where, at $t = \tau^A_{j,s} + 1$, $E_{j,s,t-1} = E^A_{j,s}$, as the initial SOC condition at EV arrival, whereas at $t = \tau^L_{j,s}$, $E_{j,s,t} = E^L_{j,s}$, the final desired SOC level at EV leaving. It should be remarked that this formulation is based on the assumption that each EV is parked for one interval per day. In the case the daily EV usage pattern includes two (or more) parking intervals, it is dealt with as two (or more) virtual EVs with a single parking interval.

Technical limits of the *j*-th EV, valid during parking interval, involve constraints on SOC and power levels:

$$0 \le P^c_{j,s,t} \le \overline{P}^c_j \cdot b_{j,s,t}. \tag{7.a}$$

$$0 \le P^d_{j,s,t} \le \overline{P}^d_j \cdot \left(1 - b_{j,s,t}\right). \tag{7.b}$$

$$\underline{v}_j \le E_{j,s,t} \le \overline{v}_j. \tag{7.c}$$

As regards technologies for charging stations, the following relations (8.a)-(8.b) link maximum charge/discharge power of the *k*-th station, $\overline{P}^c_k$ and $\overline{P}^d_k$ respectively, to the levels admitted by the r-th technology, whereas the association of the *r*-th technology to the *k*-th station is ensured by (8.c). It should be noted that the case where the *r*-th EV station standard would not provide for V2G is modelled by $\Psi^d_r = 0$:

$$\overline{P}^c_k = \sum_{r \in \Omega r} b_{r,k} \cdot \Psi^c_r. \tag{8.a}$$

$$\overline{P}^d_k = \sum_{r \in \Omega r} b_{r,k} \cdot \Psi^d_r. \tag{8.b}$$

$$\sum_{r \in \Omega r} b_{r,k} = 1. \tag{8.c}$$

2.2.4. Electric vehicles station commitment

The electric vehicle commitment is aimed at scheduling the station at which each EV should be connected, creating a link between their features.

In the planning stage, the number of stations Nk to be included in the EVSI is evaluated. For each time step of each scenario, the number of parked vehicles $J_{s,t}$ is determined starting from information on $\tau^A_{j,s}$ and $\tau^L_{j,s}$. Therefore, for each scenario, the maximum number of EVs parked at the same time is obtained, and the relevant time interval is individuated:

$$\overline{J}_s = \max_t \left(J_{s,t}\right). \tag{9.a}$$

$$\overline{\tau}_s = t \ni' J_{s,t} = \overline{J}_s. \tag{9.b}$$

The number of EV stations is eventually set to the minimum necessary to cover the maximum amount of EVs parked at the same time in any scenario:

$$Nk = \max_s \overline{J}_s. \tag{9.c}$$

Moreover, EV exploitation is characterized by evaluating, for each EV in each scenario, the average power needed to reach the final state $\pi_{j,s}$:

$$\pi_{j,s} = \frac{\left|E^L_{j,s} - E^A_{j,s}\right|}{\tau^L_{j,s} - \tau^A_{j,s}}. \tag{10}$$

Preprints (www.preprints.org) | NOT PEER-REVIEWED | Posted: 22 March 2019

Peer-reviewed version available at *Energies* **2019**, *12*, 1901; doi:10.3390/en12101901

Once Nk is determined, for each scenario, the EV commitment starts from the time step $\overline{\tau}_s$. The $\overline{J}_s$ EVs parked in this time step are associated to the charging stations according to a list sorted according to the index $\pi_{j,s}$: the EV with the highest index is connected to the first station, $k = 1$, and so on.

After that, the remaining $Nj - \overline{J}_s$ EVs are ordered according to the power index $\pi_{j,s}$. For each EV in this ranking, starting from the first one, the procedure tries the connection to the first available station, avoiding time superposition with the EVs previously selected.

This procedure can leave in idle state the last stations. In this way, the binary parameter $\beta_{j,k,s}$ is determined for all EVs, stations and scenarios.

For purpose of exemplification, an application of the EV station commitment procedure is reported in Appendix A.

Therefore, the amount of charge and discharge power that the *j*-th EV can exchange depends not only on the EV features, but also on the *k*-th station it is connected to in the *s*-th scenario, as follows:

$$0 \le P^c_{j,s,t} \le \overline{P}^c_k \cdot \beta_{j,k,s}. \tag{11.a}$$

$$0 \le P^d_{j,s,t} \le \overline{P}^d_k \cdot \beta_{j,k,s}. \tag{11.b}$$

2.2.4. Microgrid balance and power exchanges

The overall behaviour of the microgrid is governed by power balance relation, where the generation is represented by net PV production, ESS discharge, possible EV discharge and grid withdrawal, whereas the load includes ESS and EV charge and grid power delivery. Microgrid balance is expressed as in (12):

$$\sum_{p \in \Omega p} \varsigma^M \cdot P_{p,s,t} + \sum_{i \in \Omega i} \varsigma^H \cdot P^d_{i,s,t} + \sum_{j \in \Omega j} \varsigma^K \cdot P^d_{j,s,t} + \varsigma^F \cdot P^w_{s,t} = \sum_{i \in \Omega i} \frac{1}{\varsigma^H} \cdot P^c_{i,s,t} + \sum_{j \in \Omega j} \frac{1}{\varsigma^K} \cdot P^c_{j,s,t} + \frac{1}{\varsigma^F} \cdot P^g_{s,t}. \tag{12}$$

The power exchange across the interfacing converter should withstand specific constraints related to the installed converter size, as reported in relations (13.a)-(13.b):

$$R^F = \sum_{f \in \Omega f} W_f \cdot b_f. \tag{13.a}$$

$$\sum_{f \in \Omega f} b_f = 1. \tag{13.b}$$

The power exchange of the DC microgrid with the AC parts (either internal or external) is limited by the following relations, avoiding contemporaneous withdrawal and injection:

$$0 \le P^g_{s,t} \le \overline{P}^g \cdot b^g_{s,t}. \tag{14.a}$$

$$0 \le P^w_{s,t} \le \overline{P}^g \cdot \left(1 - b^g_{s,t}\right). \tag{14.b}$$

where $\overline{P}^g$ is a conveniently high value.

Moreover, grid exchange levels are bounded by installed converter size, therefore the following relations hold:

$$0 \le P^g_{s,t} \le R^F. \tag{15.a}$$

$$0 \le P^w_{s,t} \le R^F. \tag{15.b}$$

Peer-reviewed version available at *Energies* **2019**, *12*, 1901; doi:10.3390/en12101901

2.3. Objective and procedure formulation

The goal of DC microgrid optimal design under the EV exploitation conditions and space limitations is achieved by minimizing the total lifetime cost C_T of the EVSI:

$$C_T = C_B + C_O. \tag{16}$$

The lifetime operation cost C_O is determined by actualizing the yearly operation cost of the EVSI C_O^Y, determined by considering the occurrence of the *s*-th scenario for D_s times over one year, as follows:

$$C_O^Y = \sum_{s=1}^{Ns} D_s \cdot \sum_{t=1}^{Nt} \left[q_{s,t}^w \cdot P_{s,t}^w - \gamma_{s,t}^g \cdot P_{s,t}^g + \sum_{j \in \Omega j} \left(q_{j,s,t} \cdot P_{j,s,t}^c + \gamma_{j,s,t} \cdot P_{j,s,t}^d \right) \right]. \tag{17.a}$$

Assuming that the analyzed year replicates along all the lifetime, C_O is determined by discounting C_O^Y by the annuity factor:

$$C_O = \frac{1-(1+\alpha)^{-Ny}}{\alpha} \cdot C^y. \tag{17.b}$$

The building cost C_B is determined as the sum of purchasing and installation costs associated to each component of the microgrid, as follows:

$$C_B = C_B^P + C_B^I + C_B^K + C_B^G, \tag{18.a}$$

where the total investments for PV system, ESS devices, EV charging stations and grid connections are determined by the following (18.b)-(18.e), respectively.

$$C_B^P = \sum_{p \in \Omega p} \left(c_p \cdot R_p + \sum_{m \in \Omega m} c_m \cdot b_{m,p} \right). \tag{18.b}$$

$$C_B^I = \sum_{i \in \Omega i} \left(c_i \cdot R_i + \sum_{h \in \Omega h} c_h \cdot b_{h,i} \right). \tag{18.c}$$

$$C_B^K = \sum_{r \in \Omega r} c_r \cdot \sum_{k \in \Omega k} b_{r,k}. \tag{18.d}$$

$$C_B^G = \sum_{f \in \Omega f} \left(c_f + c^g \right) \cdot b_f. \tag{18.e}$$

Microgrid optimal design problem can be synthesized in the following Mixed Integer Linear Programming formulation:

$$\begin{aligned} &\min C_T(\mathbf{x}) \\ &\text{s.t.} \begin{cases} g(\mathbf{x}) = 0 \\ h(\mathbf{x}) \le 0 \\ \underline{\mathbf{x}} \le \mathbf{x} \le \overline{\mathbf{x}} \end{cases}, \end{aligned} \tag{19}$$

where equalities $g(\mathbf{x}) = 0$, inequalities $h(\mathbf{x}) \le 0$ and state variable limits $\underline{\mathbf{x}} \le \mathbf{x} \le \overline{\mathbf{x}}$ include the relations reported in Section 2.2.

3. Test system

The investigation is based on the expected installation of the proposed system in the area of Bari Port Authority, Italy, where a fleet of service EV is aimed to serve utility needs. In particular, 5 EVs, with nominal size of 24 kWh and exploitable SOC range of 0.2÷0.9 p.u., are supposed to replace current fuel-based service cars. Their uses are depicted in Figure 2 and Figure 3, in terms of average

Peer-reviewed version available at Energies 2019, 12, 1901; doi:10.3390/en12101901

daily route length and average vehicle parking time, respectively. Each EV leaves the station with a SOC of 0.8 p.u.. According to these data, 5 charging stations are considered in the EVSI since all the EVs are parked at night. Meteorological data are taken from one year measurement of a weather station [31]. It can be noted that EV5 has two parking intervals, therefore they are dealt with separately in the procedure, just as there were six EVs.

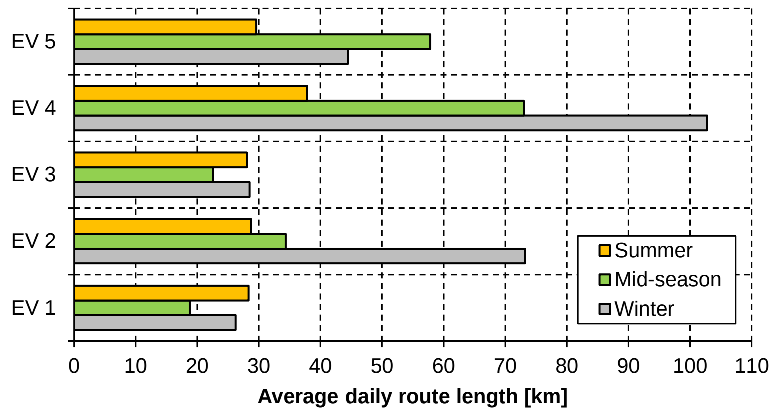

Figure 2. Average route length for the considered vehicle fleet.

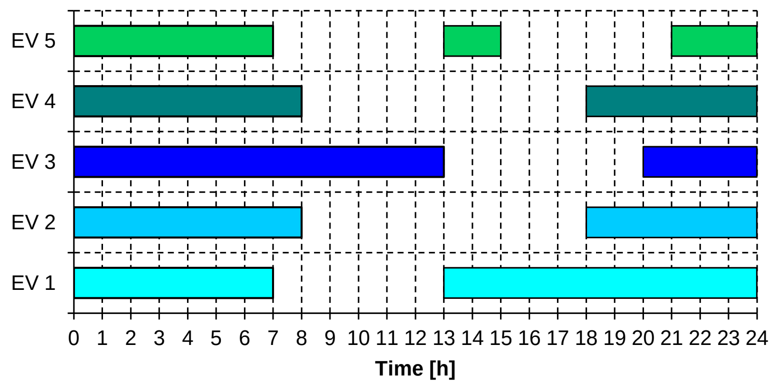

Figure 3. Average parking time for the considered vehicle fleet.

The collected data on vehicle usage and weather conditions for the reference year are divided in $Ns = 9$ scenarios, according to seasons and weather conditions, as detailed in Table 1 where the numeration and occurrence times D_s are reported. Within each scenario, a proper ratio of working days and holydays is applied. Two kinds of PV panels and three battery typologies are exploitable, and their features are synthesized in Tables 2 and 3, respectively. Available room for their installation is limited by $S_k = 15$ m², $S^{tot} = 120$ m², $V^{tot} = 2$ m³. Moreover, different converter sizes are considered, as reported in Table 4, where efficiency values and installation costs are shown as well. The latter are estimated by proper linear cost functions according to converter size, obtained from an ad hoc market investigation.

Table 1. Scenario numeration and occurrence times.

Season	Weather conditions					
	Sunny		Cloudy		Rainy	
	Scen.	D_s	Scen.	D_s	Scen.	D_s
Winter	1	13	2	46	3	31
Mid-season	4	78	5	69	6	35
Summer	7	64	8	25	9	4

Peer-reviewed version available at Energies 2019, 12, 1901; doi:10.3390/en12101901

Table 2. PV technologies characterization.

Technology	M_p [kW]	η_p^{std}	c_p [€/kW]
Monocrystalline	0.195	0.153	1514
Polycrystalline	0.245	0.148	1416

Table 3. ESS technologies characterization.

Technology	M_i [kWh]	η_i^c, η_i^d	$\overline{e}_i, \underline{e}_i$	δ_i	ω_i^c, ω_i^d	z_i [%/h] [32]	c_i [€/kWh]
LiPo	3.7	0.95	1 / 0.2	561.2	0.5 / 0.5	0.020	175
ZEBRA	19.8	0.92	1 / 0.2	183.0	0.66 / 0.66	0.250	250
Li-Ion	2.0	0.95	1 / 0.2	39.2	0.59 / 0.59	0.008	300

Table 4. Converter technologies features.

Converter type	Sizes [kW]	Efficiency [33]	Installation cost [€]
DC/DC monodir. (PV)	5, 10, 20, 30	$\zeta^M = 0.975$	$c_m = 93.247 \cdot W_m + 9531$
DC/DC bidir. (CS)	10, 20	$\zeta^K = 0.970$	$c_r = 86.713 \cdot \Psi_r^c + 7104$
DC/DC bidir. (ESS)	10, 20, 30, 60	$\zeta^H = 0.970$	$c_h = 95.832 \cdot W_i + 9498$
Two-port AC/DC	10, 20, 30, 60	$\zeta^F = 0.960$	$c_f = 41.562 \cdot W_f + 2183$

The AC grid connection cost c^g is fixed at 125 €/kWh. The cost of electricity withdrawal from the grid $q_{s,t}^w$ varies for hours and scenarios, in the range 0.14÷0.19 €/kWh, whereas unit revenue for electric energy delivery $\gamma_{s,t}^g$ is in the range 0.025÷0.055 €/kWh [34]. EV charging cost $q_{j,s,t}$ is fixed at 0.05 €/kWh according to values for wearing cost [35], whereas EV discharge is not priced ($\gamma_{j,s,t} = 0$). EVSI lifetime Ny is assumed equal to 20 years, with discount rate α equal to 0.05.

4. Results and discussion

The procedure is implemented in MatLAB2015b® framework, and solved by means of *intlinprog* function, exploiting branch and bound technique. Simulations are carried out on a workstation HP Z440 equipped with Intel Xeon 3.50 GHz processor with 16 GB RAM.

In Table 5, the values of average power $\pi_{j,s}$ are synthesized. It can be noted that the values are quite low, seldom exceeding 1 kW, therefore the choice of the minimum size for station, is expected.

Table 5. Average power needed to cover EV mobility needs [kW].

	Scenarios								
EVs	1	2	3	4	5	6	7	8	9
EV1	0.10	0.13	0.08	0.07	0.08	0.07	0.11	0.12	0.09
EV2	0.43	0.35	0.36	0.17	0.20	0.14	0.13	0.11	0.14
EV3	0.10	0.08	0.14	0.07	0.11	0.10	0.11	0.05	0.10
EV4	0.47	0.46	0.55	0.28	0.45	0.36	0.17	0.21	0.23
EV5 (night)	0.14	0.13	0.15	0.17	0.30	0.13	0.1	0.13	0.07
EV5 (mid-day)	0.98	0.93	1.06	1.16	2.12	0.89	0.68	0.90	0.47

Preprints (www.preprints.org) | NOT PEER-REVIEWED | Posted: 22 March 2019

Peer-reviewed version available at *Energies* **2019**, *12*, 1901; doi:10.3390/en12101901

As regards EV-station commitment, the results are illustrated in Figure 4. It can be seen that the 5 EVs are associated to stations according to the order of $\pi_{j,s}$, since they are contemporaneously parked during the night. Moreover, since EV4 always has the maximum power demand, it is always associated to the first station. The mid-day parking interval of EV5 is associated to the first available station.

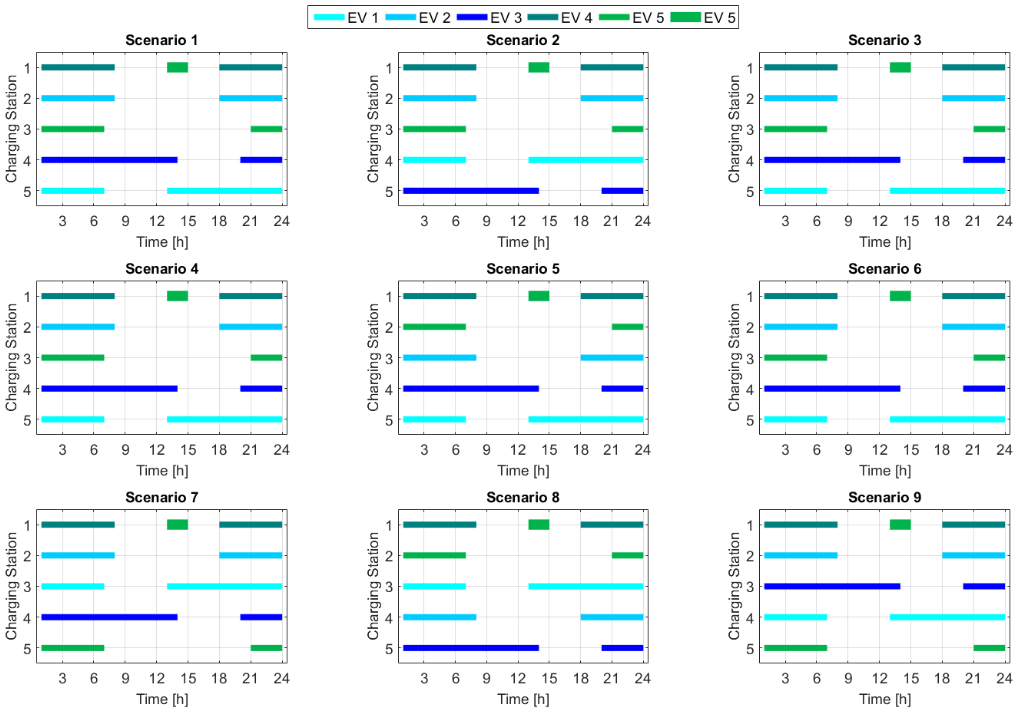

Figure 4. EV-station commitment for each scenario.

A synthesis of the obtained results is reported in Table 6 for installations, where unexploited technologies among the available ones described in Section 2 are not reported for purpose of brevity. It can be seen that the goal of minimum economic effort is reached by exploiting the lower size of EV stations, polycrystalline PV modules and, where deemed necessary, LiPo batteries. No ESS installation is provided, due to the high installation cost of the converter and to the possibility of exploiting EVs for storage tasks thanks to V2G stations.

Table 6. Optimal sizing results: installation sizes.

Device or technology	number	kW	kWh
PV polycrystalline modules	46	11.27	
ESS LiPo batteries	0		0
Bidirectional EV stations	5	10 (each)	
Grid connection	1	10	
PV converter	1	20	
ESS converter	0		
Two-port grid converter	1	10	

Yearly energy exchange levels are reported in Figure 5, where it can be seen that, out of the total value of 19.86 MWh, PV covers 76.1% of production, leaving 16.6% to EV discharge and 7.3% to grid withdrawal. Whereas, total consumption is composed by EV charge for 58.1% grid injection for 35.9% and losses represent 6.0%. Moreover, the ratio of grid withdrawal on grid injection is 0.203, whereas the ratio of EV discharge on EV charge is 0.285, showing a preference to EV as power storage, when present.

Economic results are synthesized in Table 7. It can be noted that the building cost represents almost 93% of the objective function. Operation costs are very limited, reaching 518.5 € yearly.

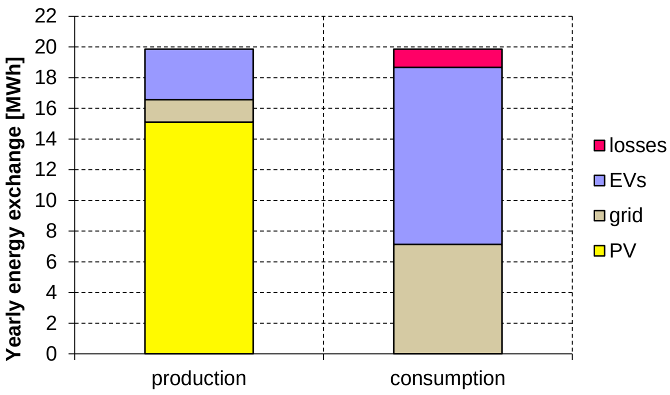

Figure 5. Optimal sizing results: yearly energy exchanges.

Table 7. Optimal sizing results: economic yields.

Cost component	Value [€]
Building cost C_B	83483.6
Yearly operation cost C_O^Y	518.5
Lifetime operation cost C_O^Y	6449.8
Total EVSI cost C_T	89933.4

For sake of exemplification, trends in all the analyzed scenarios of electric power balance, of EV power exchange levels and of state of charge (SOC) of EVs are reported in Figures 6-8, respectively. It can be seen that, an amount of grid power delivery is observed in all scenarios except rainy days of Scenario 3 and Scenario 6, where the limited PV production is fully exploited to charge EVs. Whereas, grid power withdrawal is registered only in five scenarios, and is not present in summer. A limited amount of EV discharge is observed in all scenarios, mostly related to EV 3 and EV 1 due to their parking time in intervals with higher PV production, allowing SOC increase beyond the final value or a decrease towards the minimum. However, EV discharge is present only to exchange power with other EVs.

As regards computational performances, the whole procedure took 40.0 seconds to reach the solution.

Peer-reviewed version available at *Energies* **2019**, *12*, 1901; doi:10.3390/en12101901

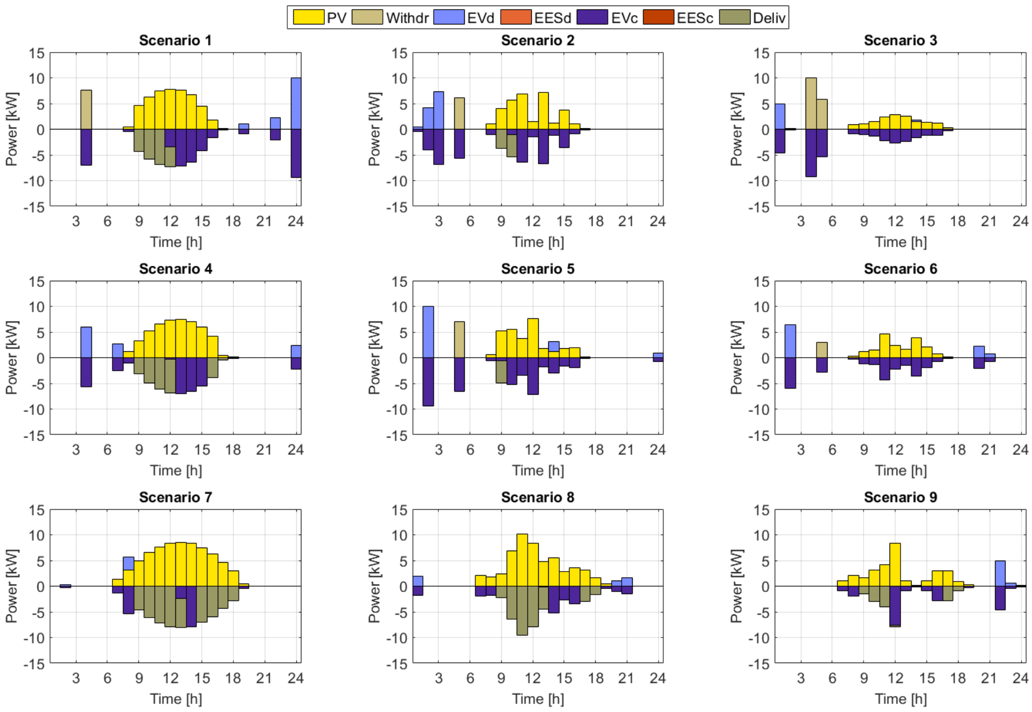

Figure 6. Electric power balance for each scenario.

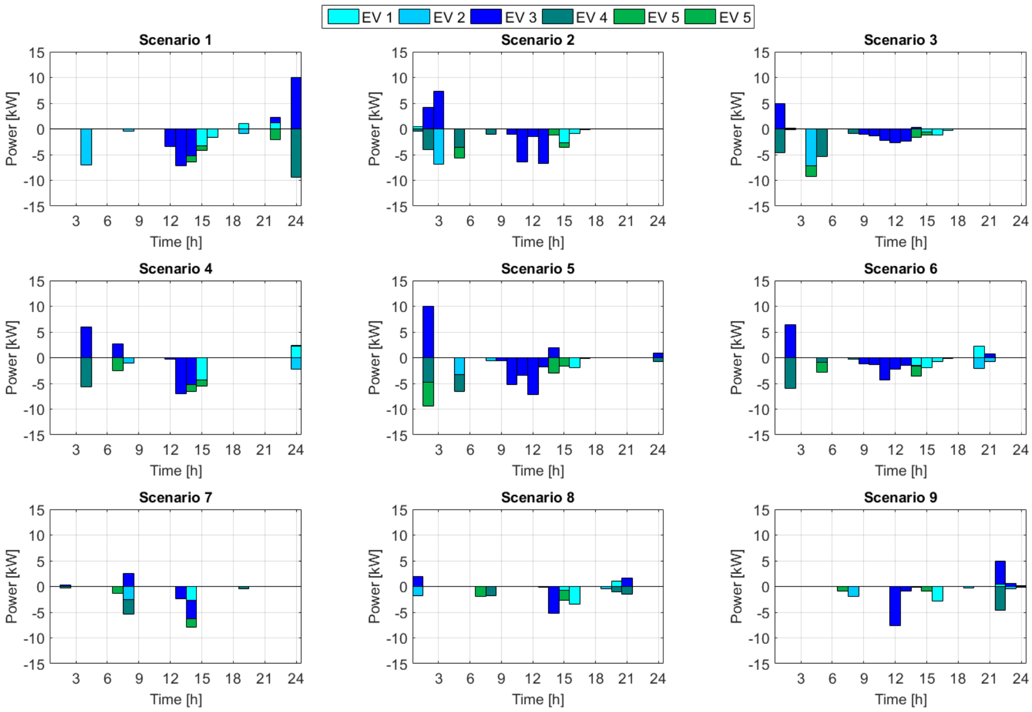

Figure 7. EV power levels for each scenario.

Peer-reviewed version available at Energies 2019, 12, 1901; doi:10.3390/en12101901

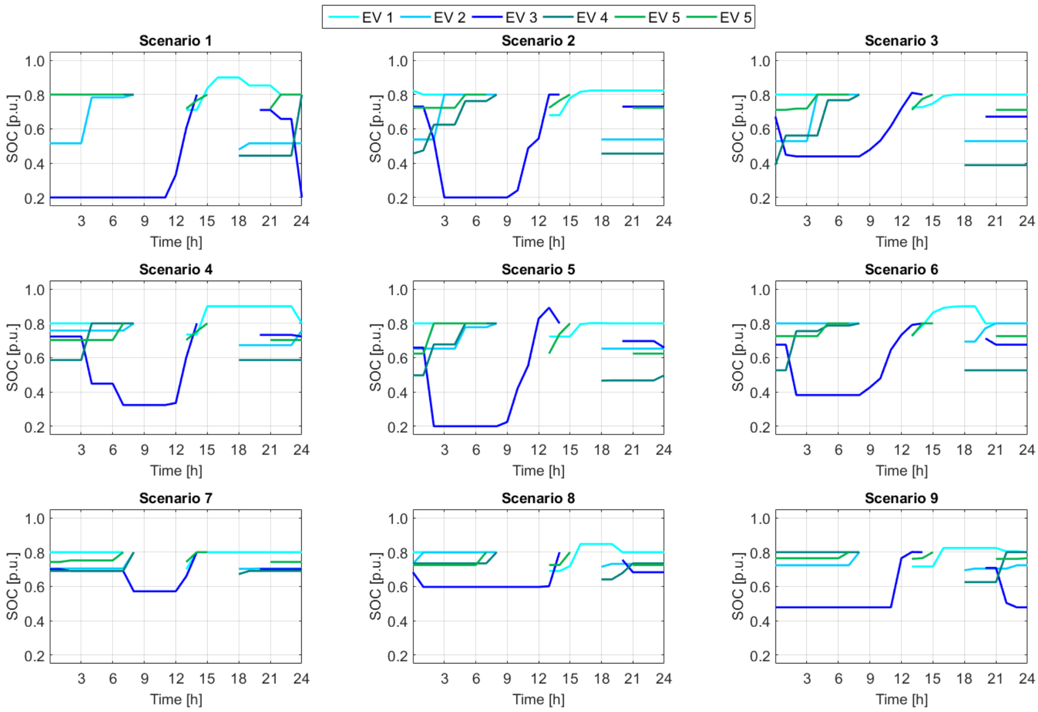

Figure 8. State of charge of EVs for each scenario.

5. Conclusions

In this paper, a mixed-integer linear optimization methodology has been carried out for techno-economic sizing of a DC-microgrid including PV canopy, EV charging stations with V2G features and battery-based ESS with the connection to AC distribution network. The procedure is based on the definition of operating scenarios according to weather conditions and EV uses, and involves a specific model for the commitment of EV connection to charging station according to EV planned mobility need. The proposed approach has been applied to a case study of envisaged EV service fleet for Bari Port Authority. Results have shown that the presence of ESS can be hindered by the higher cost due to dedicated converters. The effectiveness of the EV-station commitment strategy has been verified. Future work will deal with the investigation of further DC microgrid configurations, as well as the influence of reliability figures on the selection of the technical solutions.

Author Contributions: M.D., G.F. and R.S. provided for research framework and literature analysis; A.B., G.F. and M.T. developed the model; M.D., I.F. and R.S. cared for data collection; A.B., I.F. and G.F. set up the program and performed the simulations; A.B., I.F. and M.T. formalized the nomenclature; A.B. and G.F. wrote the paper; M.D. and M.T. edited the paper; M.D. and M.T. cared for relation with funding project.

Funding: This document has been created in the context of the CONNECT project. The CONNECT project has received funding from the ECSEL Joint Undertaking under Grant Agreement n° 737434-2 and from the national programmes/funding authorities of Germany, Italy, Slovakia, Spain and The Netherlands. The ECSEL JU has no liability in respect of this document, which is merely representing the authors' view.

Conflicts of Interest: The authors declare no conflict of interest. The funders had no role in the design of the study; in the collection, analyses, or interpretation of data; in the writing of the manuscript, or in the decision to publish the results.

Preprints (www.preprints.org) | NOT PEER-REVIEWED | Posted: 22 March 2019

Peer-reviewed version available at *Energies* **2019**, *12*, 1901; doi:10.3390/en12101901

Nomenclature

Indices (subscripts)

t	Time step
s	Scenario
p	Photovoltaic (PV) technology
i	Energy storage system (ESS) technology
j	Electric vehicle (EVs)
k	EV station
r	Charging/V2G technology standard
m	PV converter
h	ESS converter
f	AC/DC grid connection converter

Sets and general definitions

Nt	Total number of time steps
Ns	Total number of scenarios
Ωp	Set of available PV technologies (total number Np)
Ωi	Set of available ESS technologies (total number Ni)
Ωj	Set of EVs (total number Nj)
Ωk	Set of charging stations (total number Nk)
Ωr	Set of EV charging/V2G standards (total number Nr)
Ωm	Set of PV converters (total number Nm)
Ωh	Set of ESS converters (total number Nh)
Ωf	Set of AC/DC converters (total number Nf)
Ny	Total number of years of the analysis
α	Discount rate
Δt	Duration of each time step [h]
D_s	Number of occurrences of the s-th scenario in a year

Cost breakdown

C_T	Total lifetime cost of the microgrid [€]
C_B	Total building cost of the microgrid [€]
C_B^P	Building cost of the PVs and their connection [€]
C_B^I	Building cost of the ESSs and their connection [€]
C_B^K	Building cost of the EV stations and their connection [€]
C_B^G	Building cost of DC microgrid internal connections and of AC network interface [€]

Peer-reviewed version available at *Energies* **2019**, *12*, 1901; doi:10.3390/en12101901

C_O	Total operation cost of the microgrid [€]
C_O^Y	Yearly operation cost of the microgrid [€]

PV system parameters

S_k	parking surface for each charging station [m²]
S^{tot}	total available surface for EV parking roofs [m²]
η_p^{std}	standard efficiency of the *p*-th PV technology
$\eta_{p,s,t}$	efficiency of the *p*-th PV technology in the *t*-th time step of the *s*-th scenario
$G_{p,s,t}$	solar radiation on the *p*-th PV at the *t*-th time step in the *s*-th scenario [kW/m²]
M_p	Unit power of the *p*-th PV technology panel [kW]
W_m	Installed power for the *m*-th PV converter [kW]
ζ^M	PV converter efficiency
c_p	Investment cost of a PV panel of the *p*-th technology [€/kW]
c_m	Investment cost of the *m*-th PV converter [€]

Energy storage system parameters

η_i^c, η_i^d	charge and efficiency of the *i*-th ESS
$\overline{e}_i, \underline{e}_i$	maximum and minimum allowable state of charge SOC for the *i*-th ESS, in p.u. of installed size
$E_{i,s,0}$	initial condition of SOC for the *i*-th ESS in the *s*-th scenario [kWh]
V^{tot}	total available volume for hosting ESS [m³]
δ_i	specific energy per unit of volume for the *i*-th ESS [kWh/m³]
φ_i^c, φ_i^d	energy-to-power ratio, of the *i*-th ESS in charge and discharge conditions [kWh/kW]
z_i	self-discharge rate of the *i*-th ESS
M_i	Unit size of the *i*-th ESS technology module [kWh]
W_h	Installed power for the *h*-th ESS converter [kW]
ζ^H	ESS converter efficiency
c_i	Investment cost of an ESS module for the *i*-th technology [€/kWh]
c_h	Investment cost of the *h*-th ESS converter [€]

Electric vehicles and stations parameters

ρ_j^c, ρ_j^d	charge and efficiency of the *j*-th EV
$\overline{v}_j, \underline{v}_j$	maximum and minimum SOC for the *j*-th EV
$\tau_{j,s}^A, \tau_{j,s}^L$	arrival and leaving time step of the *j*-th EV at the station in the *s*-th scenario
$E_{j,s}^A, E_{j,s}^L$	SOC at arrival and leaving time for the *j*-th EV in the *s*-th scenario [kWh]
$J_{s,t}$	number of parked EVs at the *t*-th time step in the *s*-th scenario
$\overline{J}_s$	maximum number of parked EVs in the *s*-th scenario

Peer-reviewed version available at Energies 2019, 12, 1901; doi:10.3390/en12101901

$\bar{\tau}_s$	time step with the maximum number of parked EVs in the *s*-th scenario
$\bar{P}_j^c, \bar{P}_j^d$	maximum charge and discharge power of the *j*-th EV [kW]
Ψ_r^c, Ψ_r^d	maximum charge and discharge power of the *r*-th charging/V2G standard [kW]
$\pi_{j,s}$	Average power needed to charge the *j*-th EV in the *s*-th scenario over the defined parking time
$\beta_{j,k,s}$	Binary value assigning the connection of the *j*-th EV at the *k*-th station in the *s*-th scenario
ζ^K	charging station efficiency
c_r	Investment cost in the *r*-th technology for vehicle charging/V2G station [€]
$q_{j,s,t}, \gamma_{j,s,t}$	Cost for EV charge and EV discharge at the *t*-th time step in the *s*-th scenario [€/kWh]

Grid connection parameters

W_f	Nominal power of the *f*-th AC/DC converter [kW]
ζ^F	AC/DC converter efficiency
$\bar{P}^g$	Maximum exchangeable power at PCC, in either injection or withdrawal [kW]
$q_{s,t}^w$	Cost for electric energy purchase from the grid at PCC at the t-th time step in the *s*-th scenario [€/kWh]
$\gamma_{s,t}^g$	Revenue for electric energy delivery to the grid at PCC at the t-th time step in the *s*-th scenario [€/kWh]
c_f	Investment cost of the *f*-th grid converter [€]
c^g	Investment cost of AC grid connection [€]

Real State Variables

$P_{s,t}^w$	Amount of power withdrawal from the distribution grid at the *t*-th time step in the *s*-th scenario [kW]
$P_{s,t}^g$	Amount of power injected into the distribution grid at the *t*-th time step in the *s*-th scenario [kW]
$P_{i,s,t}^c$	Charge power for the *i*-th ESS at the *t*-th time step in the *s*-th scenario [kW]
$P_{i,s,t}^d$	Discharge power for the *i*-th ESS at the *t*-th time step in the *s*-th scenario [kW]
$E_{i,s,t}$	State of charge (SOC) of the *i*-th ESS at the *t*-th time step in the *s*-th scenario [kWh]
$P_{j,s,t}^c$	Charge power for the *j*-th EV at the *t*-th time step in the *s*-th scenario [kW]
$P_{j,s,t}^d$	Discharge power for the *j*-th EV at the *t*-th time step in the *s*-th scenario [kW]
$E_{j,s,t}$	State of charge (SOC) of the *j*-th EV at the *t*-th time step in the *s*-th scenario [kWh]
$\bar{P}_k^c$	maximum charge power at *k*-th station
$\bar{P}_k^d$	maximum discharge power at *k*-th station
R_p	Installed power for the *p*-th PV technology [kW]

Preprints (www.preprints.org) | NOT PEER-REVIEWED | Posted: 22 March 2019

Peer-reviewed version available at *Energies* **2019**, *12*, 1901; doi:10.3390/en12101901

R_i Installed size for the i-th ESS technology [kWh]

R^F Installed power for the grid converter [kW]

Integer State Variables:

$b^g_{s,t}$ Variable to select power withdrawal or injection from the AC grid at the t-th time step in the s-th scenario

$b_{i,s,t}$ Variable to select either charge or discharge for the i-th ESS at the t-th time step in the s-th scenario

$b_{j,s,t}$ Variable to select either charge or discharge for the j-th EV at the t-th time step in the s-th scenario

$b_{r,k}$ Variable linking the k-th station to the r-th standard for charging/V2G it is equipped with

n_p Number of modules for the p-th PV technology

n_i Number of battery modules of the i-th ESS technology

$b_{m,p}$ Binary variable indicating if the m-th PV converter is exploited for the p-th PV technology

$b_{h,i}$ Binary variable indicating if the i-th ESS converter is exploited for the i-th ESS technology

b_f Binary variable to select the installation of the f-th two-port AC/DC grid converter

Appendix A – An example of EV and station commitment procedure

Let us suppose that a group of 15 EVs should be managed by a microgrid including $Nk = 7$ stations, according to a scenario of utilization. In Figure A1, they are numbered according to the power index $\pi_{j,s}$ and their parking times are represented. It can be seen that, in this case, a maximum of $\overline{J}_s = 6$ EVs are contemporaneously parked at $\overline{\tau}_s = 17$, namely, EVs 2, 3, 7, 9, 11, 15. These EVs are associated to the first 6 stations in this order.

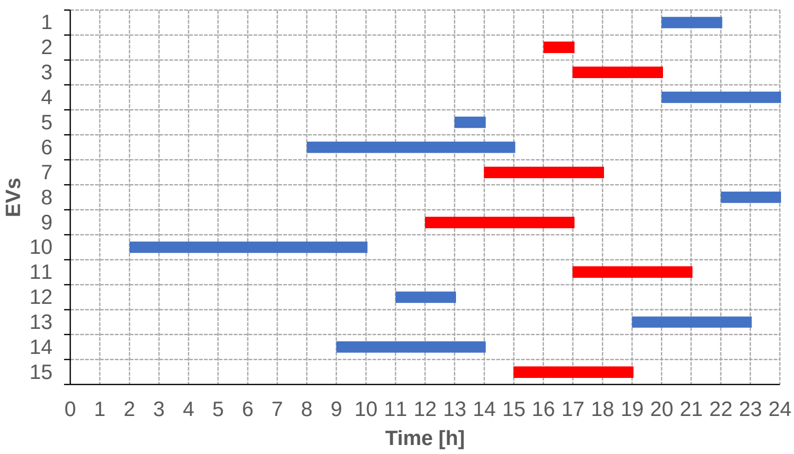

Figure A1. Example of EV and station commitment. Parking time of 15 EVs – in red the EVs parked at hour 17.

Peer-reviewed version available at *Energies* **2019**, *12*, 1901; doi:10.3390/en12101901

Therefore, the remaining EVs are committed, according to the numbering order. In particular, EV 1 finds station 1 free at its parking time, and is settled there. Whereas, EV 4 cannot be connected to station 1, busy due to the presence of EV 1, nor to station 2, where EV 2 is connected, but it finds station 3 free. Proceeding in this way, the final EV-station commitment is obtained, as reported in Table A1, where bold numbers report EVs parked at hour 17. It can be noted that station 7 is unexploited.

Table A1. Example of EV and station commitment. Allocation of all EVs at microgrid stations.

stations \ hours	**1**	**2**	**3**	**4**	**5**	**6**	**7**	**8**	**9**	**10**	**11**	**12**	**13**	**14**	**15**	**16**	**17**	**18**	**19**	**20**	**21**	**22**	**23**	**24**
1		10	10	10	10	10	10	10	10	10			5	5		**2**	**2**			1	1	1		
2								6	6	6	6	6	6	6	6		**3**	**3**	**3**	**3**		8	8	8
3											12	12	12	**7**	**7**	**7**	**7**	**7**		4	4	4	4	4
4												**9**	**9**	**9**	**9**	**9**	**9**		13	13	13	13	13	
5									14	14	14	14	14	14			**11**	**11**	**11**	**11**	**11**			
6															**15**	**15**	**15**	**15**	**15**					
7																								

In this way, for the selected scenario, the binary parameter $\beta_{j,k,s}$ is determined as reported in Table A2, where values equal to 0 are not reported for sake of readability.

Table A2. Example of EV and station commitment. Values of the binary parameter EV-station.

stations \ EVs	**1**	**2**	**3**	**4**	**5**	**6**	**7**	**8**	**9**	**10**	**11**	**12**	**13**	**14**	**15**
1	1	1			1					1					
2			1			1		1							
3				1			1					1			
4									1				1		
5											1			1	
6															1
7															

References

1. P. Vithayasrichareon, G. Mills, I. F. MacGill, “Impact of Electric Vehicles and Solar PV on Future Generation Portfolio Investment”, *IEEE Trans. Sust. Energy*, vol. 6, no. 3, July **2015**, pp. 899-908 (DOI: 10.1109/TSTE.2015.2418338).
2. A. Schroeder, T. Traber, “The economics of fast charging infrastructure for electric vehicles”, *Energy Policy*, vol. 43, Apr. **2012**, pp. 136-144 (DOI: 10.1016/j.enpol.2011.12.041).
3. R. Abousleiman, R. Scholer, “Smart Charging: System design and implementation for interaction between plug-in electric vehicles and the power grid”, *IEEE Trans. Transp. Electrif.*, vol. 1, no. 1, June **2015**, pp. 18-25 (DOI: 10.1109/TTE.2015.2426571).
4. J. Garcia-Villalobos, I. Zamora, J.I. San Martin, F.J. Asensio, V. Aperribay, “Plug-in electric vehicles in electric distribution networks: a review of smart charging approaches”, *Renew. Sust. Energy Reviews*, vol. 38, Oct. **2014**, pp. 717-731 (DOI: 10.1016/j.rser.2014.07.040).
5. P. You, Z. Yang, “Efficient Optimal Scheduling of Charging Station with Multiple Electric Vehicles via V2V”, Proc. of 2014 IEEE Int. Conf. on Smart Grid Communications, pp. 716-721 (DOI: 10.1109/SmartGridComm.2014.7007732).

Peer-reviewed version available at *Energies* **2019**, *12*, 1901; doi:10.3390/en12101901

6. A. R. Bhatti, Z. Salam, M.J.B.A. Aziz, K.P. Yee, R.H. Ashique, "Electric vehicles charging using photovoltaic: Status and technological review", *Renew. Sust. Energy Reviews*, vol. 54, pp. 54-47, **2016** (DOI: 10.1016/j.rser.2015.09.091).
7. W. Tian, W. Jiang, M. Shahidehpour, M. Krishnamurthy, "Vehicle charging stations with solar canopy: A realistic case study within a smart grid environment", Proc. of 2014 IEEE Transportation Electrification Conf. and Expo, pp. 1-6, (DOI: 10.1109/ITEC.2014.6861801).
8. M. Brenna, A. Dolara, F. Foiadelli, S. Leva, M. Longo, "Urban scale photovoltaic charging stations for electric vehicles", *IEEE Trans. Sust. Energy*, Vol. 5, no. 4, Oct. **2014**, pp. 1234-1241 (DOI: 10.1109/TSTE.2014.2341954).
9. U.C. Chukwu, S.M. Mahajan, "V2G parking lot with PV rooftop for capacity enhancement of a distribution system", *IEEE Trans. Sust. Energy*, Vol. 5, no. 1, January **2014**, pp. 119-127 (DOI: 10.1109/TSTE.2013.2274601).
10. P.J. Tulpule, V. Marano, S. Yurkovich, G. Rizzoni, "Economic and environmental impacts of a PV powered workplace parking garage charging station", *Applied Energy*, vol. 108, **2013**, pp. 323-332 (DOI: 10.1016/j.apenergy.2013.02.068).
11. F. Fattori, N. Anglani, G. Muliere, "Combining photovoltaic energy with electric vehicles, smart charging and vehicle-to-grid", *Solar Energy*, vol. 110, **2014**, pp. 438-451 (DOI: 10.1016/j.solener.2014.09.034).
12. D. Sbordone, I. Bertini, B. Di Pietra, M.C. Falvo, A. Genovese, L. Martirano, "EV fast charging stations and energy storage technologies: A real implementation in the smart micro grid paradigm", *Electric Power Systems Research*, vol. 120, **2015**, pp. 96-108 (DOI: 10.1016/j.epsr.2014.07.033).
13. I. Safak Bayram, G. Michailidis, M. Devetsikiotis, S. Bhattacharya, A. Chakrabortty, F. Granelli, "Local energy storage sizing in plug-in hybrid electric vehicle charging stations under blocking probability constraints", Proc. of 2011 IEEE SmartGridComm Conference, pp. 78-83 (DOI: 10.1109/SmartGridComm.2011.6102396).
14. G.R. Chandra Mouli, P. Bauer, M. Zeman, "System design for a solar powered electric vehicle charging station for workplaces", *Applied Energy*, vol. 168, pp. 434-443, **2016** (DOI: 10.1016/j.apenergy.2016.01.110).
15. G. Preetham, W. Shireen, "Photovoltaic charging station for plug-in hybrid electric vehicles in a smart grid environment", proc. of 2012 IEEE PES ISGT Conference, 16-20 Jan. 2012, pp. 1-8 (DOI: 10.1109/ISGT.2012.6175589).
16. B. Aluisio, M. Dicorato, G. Forte, M. Trovato, "A Monte-Carlo Based procedure for optimal sizing of integrated Electric Vehicle Supply Infrastructure", Proc. of IEEE ISGT Europe 2017 Conference, 26-29 Sept. 2017, Turin, Italy, pp. 1-6 (DOI: 10.1109/ISGTEurope.2017.8260188).
17. B. Aluisio, M. Dicorato, I. Ferrini, G. Forte, M. Trovato, "AC and DC solutions for Electric Vehicle microgrid: sizing and reliability analysis", Proc. of IEEE 2018 EEEIC/I&CPS Europe Int. Conf., 12-15 June 2018 Palermo, Italy, pp. 1-6 (DOI: 10.1109/EEEIC.2018.8494356).
18. R.H. Ashique, Z. Salam, M.J. Bin Abdul Aziz, A.R. Bhatti, "Integrated photovoltaic-grid dc fast charging system for electric vehicle: A review of the architecture and control", *Renew. Sust. Energy Reviews*, vol. 69, **2017**, pp. 1243-1257 (DOI: 10.1016/j.rser.2016.11.245).
19. S. Kaur, T. Kaur, R. Khanna, P. Singh, "A State of the art of DC microgrids for Electric Vehicle Charging", proc. of 4th IEEE ISPC 2k17 Conference, Sept. 21-23 2017, Solan, India, pp. 381-386 (DOI: 10.1109/ISPCC.2017.8269708).
20. Y. Chen, W. Wei, F. Zhang, C. Liu, C. Meng, "Design of PV Hybrid DC/AC Microgrid for Electric Vehicle Charging Station", Proc. of 2017 ITEC Asia-Pacific Conference, 7-10 Aug. 2017, Harbin, China, pp. 1-6 (DOI: 10.1109/ITEC-AP.2017.8081027).
21. Y.-T. Liao, C.N. Lu, "Dispatch of EV Charging Station Energy Resources for Sustainable Mobility", *IEEE Trans. Transp. Electrif.*, vol. 1, no. 1, June **2015**, pp. 86-93 (DOI: 10.1109/TTE.2015.2430287).
22. W. Tushar, C. Yuen, S. Huang, D.B. Smith, H.V. Poor, "Cost Minimization of Charging Stations With Photovoltaics: An Approach With EV Classification", *IEEE Trans. Intell. Transp. Syst.*, Vol. 17, no. 1, January **2016**, pp. 156-169 (DOI: 10.1109/TITS.2015.2462824).
23. X. Lu, N. Liu, Q. Chen, J. Zhang, "Multi-objective Optimal Scheduling of a DC Micro-grid Consisted of PV System and EV Charging Station", Proc. of 2014 IEEE ISGT Asia Conf., pp. 487-491 (DOI: 10.1109/ISGT-Asia.2014.6873840).
24. F. Marra, C. Traeholt, E. Larsen, "Planning future electric vehicle central charging station connected to low-voltage distribution network", Proc. of PEDG 2012, Aalborg, Denmark, pp. 636-641 (DOI: 10.1109/PEDG.2012.6254069).

25. C. Corchero, M. Cruz-Zambrano, F.-J. Heredia, J.-I. Caro, L. Igualada-Gonzalez, A. Romero-Ortega, “Optimal sizing of microgrid, a fast charging station case”, Proc. of 2012 European Energy market (EEM) Conf., 10-12 May 2012, pp. 1-6 (DOI: 10.1109/EEM.2012.6254677).
26. N. Machiels, N. Leemput, J. Van Roy, F. Geth, J. Driesen, “Design criteria for electric vehicle fast charge infrastructure based on Flemish mobility behavior”, *IEEE Trans. Smart Grid*, vol. 5, no. 1, Jan. **2014**, pp. 320-327 (DOI: 10.1109/TSG.2013.2278723).
27. J. Ugirumurera, Z. J. Haas, “Optimal capacity sizing for completely green charging systems for electric vehicles”, *IEEE Trans. Transp. Electrif.*, vol. 3, no. 3, Sept. **2017**, pp. 565-577 (DOI: 10.1109/TTE.2017.2713098).
28. C. Wang, B. Jiao, L. Guo, K. Yuan, B. Sun, “Optimal planning of stand-alone microgrids incorporating reliability”, *J. Mod. Power Syst. Clean Energy*, vol. 2, no. 3, **2014**, pp. 195-205 (DOI 10.1007/s40565-014-0068-9).
29. E. X. Dominguez, P. Arboleya, “Reliability assessment in photovoltaic nanogrids by means of principal components analysis” Proc. of IEEE 2016 PES General Meeting, 17-21 July 2016, Boston, MA, USA, pp. 1-5 (DOI: 10.1109/PESGM.2016.7741155).
30. J. A. Duffie, W. A. Beckman, “Solar Engineering of Thermal Processes - Fourth Edition”, John Wiley & Sons, 2013.
31. www.wunderground.com
32. G. L. Soloveichik, “Battery technologies for Large-Scale Stationary Energy Storage”, *Annu. Rev. Chem. Biomol. Eng*, **2011**, 2: 503-527 (DOI: 10.1146/annurev-chembioeng-061010-114116).
33. H. Fathabadi, “Novel high efficiency DC/DC boost converter for using in photovoltaic systems”, *Solar Energy*, vol. 125, Feb. **2016**, pp. 22-31 (DOI: 10.1016/j.solener.2015.11.047).
34. ARERA, the Italian Regulatory Authority for Energy, Networks and Environment, Electricity prices for customers, (in Italian), https://www.arera.it/it/prezzi.htm#
35. B. Aluisio, A. Conserva, M. Dicorato, G. Forte, M. Trovato, “Optimal operation planning of V2G-equipped Microgrid in the presence of EV aggregator”, *Electric Power Systems Research*, Vol. 152, Nov. **2017**, pp. 295-305 (DOI: 0.1016/j.epsr.2017.07.015).